

**Search for temperature and  $N/Z$  dependent effects in the decay of  $A=98$  compound nuclei**

S. Moretto,<sup>1</sup> D. Fabris,<sup>1</sup> M. Lunardon,<sup>1</sup> S. Pesente,<sup>1</sup> V. Rizzi,<sup>1</sup> G. Viesti,<sup>1</sup> M. Barbui,<sup>2</sup> M. Cinausero,<sup>2</sup> E. Fioretto,<sup>2</sup> G. Prete,<sup>2</sup> A. Brondi,<sup>3</sup> E. Vardaci,<sup>3</sup> F. Lucarelli,<sup>4</sup> A. Azhari,<sup>5</sup> X. D. Tang,<sup>5</sup> K. Hagel,<sup>5</sup> Y. Ma,<sup>5</sup> A. Makeev,<sup>5</sup> M. Murray,<sup>5</sup> J. B. Natowitz,<sup>5</sup> L. Qin,<sup>5</sup> P. Smith,<sup>5</sup> L. Trache,<sup>5</sup> R. E. Tribble,<sup>5</sup> R. Wada,<sup>5</sup> and J. Wang<sup>5</sup>

<sup>1</sup>*Dipartimento di Fisica dell'Università and INFN Sezione di Padova, I-35131 Padova, Italy*

<sup>2</sup>*INFN Laboratori Nazionali di Legnaro, I-35020 Legnaro, Italy*

<sup>3</sup>*INFN and Dipartimento di Fisica dell'Università di Napoli, I-80125 Napoli, Italy*

<sup>4</sup>*INFN and Dipartimento di Fisica dell'Università di Firenze, I-50125 Firenze, Italy*

<sup>5</sup>*Cyclotron Institute, Texas A&M University, College Station, Texas 77843-3366, USA*

(Received 23 July 2003; published 16 April 2004)

Fusion-evaporation reactions induced by 110 MeV  $^{11}\text{B}$  and radioactive  $^{11}\text{C}$  on  $^{87}\text{Rb}$  targets have been studied by measuring evaporation residue–light particle coincidences. The proton to  $\alpha$  particle ratio in each reaction has been derived and compared with predictions from statistical model calculations. These calculations account rather well for the experimental data, when a small empirical adjustment of the emission barrier is performed, in agreement with earlier results. No evidence is found for predicted temperature and isospin modification of the binding energies. The possibility of a further study of isospin and temperature dependent effects in fusion-evaporation reactions with radioactive beams is discussed.

DOI: 10.1103/PhysRevC.69.044604

PACS number(s): 24.60.Dr, 25.70.Gh

**I. INTRODUCTION**

The temperature dependence of basic nuclear properties has been the subject of several studies in past years [1]. Compound systems at high excitation energies, such as those populated in heavy-ion reactions, offer the possibility to explore changes in the basic properties of highly excited nuclei with respect to their ground state. One of the interesting theoretical results in this field is the description of the temperature dependence of the nucleon effective mass [2] and its consequences on nuclear level densities [3]. Theoretical predictions, showing the importance of this effect at high excitation energy (i.e., about  $E_x=2$  MeV/nucleon for nuclei in the mass region  $A=160$ ) have been confirmed by a number of experimental investigations [4–6]. Such excitation energies correspond to nuclear temperature values above  $T=4$  MeV, when the relationship between excitation energy and temperature is assumed to be  $E_x=aT^2$ , with the level density parameter  $a=A/K$  MeV $^{-1}$ . More recently, the temperature dependence of the so-called  $\omega$  effective mass  $m_\omega$  has been calculated for some nuclei of astrophysical interest,  $^{98}\text{Mo}$ ,  $^{64}\text{Zn}$ , and  $^{64}\text{Ni}$  [7]. It was found that, in all cases,  $m_\omega$  decreases appreciably, already at excitation energies corresponding to temperature values below  $T=2$  MeV. The authors pointed out that this decrease should affect not only the level density but also the symmetry energy  $E_{sym}$  contribution to the binding energy, which is parametrized as

$$E_{sym} = b_{sym}(N-Z)^2/A,$$

where  $A$  is the mass of the nucleus,  $Z$  its atomic number, and  $N=A-Z$  the neutron number. We note that in this parametrization the symmetry energy term exhibits intrinsically a marked isospin dependence. The symmetry coefficient  $b_{sym}$  value is 30 MeV at  $T=0$  MeV. As discussed in detail in Ref. [7], such a dependence is of particular interest at low

temperature, since it would have a strong impact on the actual knowledge of the supernova collapse and explosion dynamics. A consistent temperature parametrization of the nuclear mass in the framework of the Thomas-Fermi model has also been proposed by Pi, Vinas, and Barranco [8] and used in modeling temperature dependent fission barriers.

From the experimental side, a simple observable, directly related to the binding energy variation through the temperature dependence of the nuclear mass, is the multiplicity of the emitted particles. In this case, the measured particle multiplicities should deviate from standard statistical model predictions, in which the usual  $T=0$  MeV masses are used. Since differences between experimental data and statistical model predictions may also result from intrinsic limitations in the model accuracy, one possible way to assess the presence of such effects is to take advantage of its predicted dependence on the  $(N-Z)^2/A$  ratio of the emitter, by studying the decay of isobars populated at the same excitation energy. New possibilities in this field are now opened by the present availability of some radioactive beams.

We report in this work a comparative study of light particle emission from the two isobars,  $^{98}\text{Mo}$  and  $^{98}\text{Tc}$ , populated, respectively, in the fusion reactions of 110 MeV  $^{11}\text{B}$  and  $^{11}\text{C}$  beams on a  $^{87}\text{Rb}$  target. The excitation energy of the compound nuclei is in both cases about 110 MeV, which corresponds to a nuclear temperature  $T\sim 3$  MeV, assuming a level density parameter value  $a=A/8$  MeV $^{-1}$ .

Although the two beams used allow a relatively limited investigation of the isospin dependent effects, this experiment contributes to the progress in this research field which is of primary interest for future radioactive ion beam (RIB) projects. Moreover it has been specifically designed to search for isospin and temperature dependent effects in the  $^{98}\text{Mo}$  nucleus, because of its astrophysical interest.

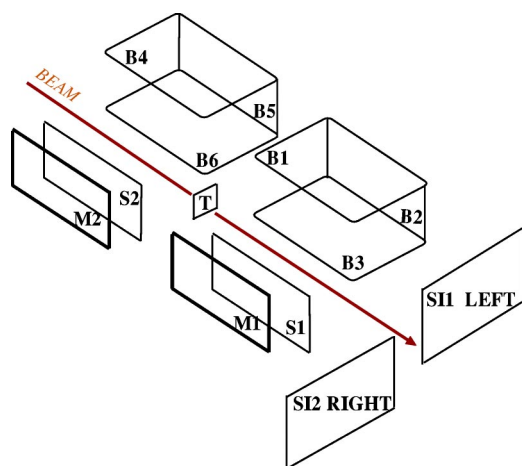


FIG. 1. (Color online) Expanded view of the experimental setup. The SI-BARREL elements are single detectors ( $300\ \mu\text{m}$  thickness,  $5 \times 5\ \text{cm}^2$  area) indicated as B1–B6. The two telescopes S1-M1 and S2-M2 are made of a transmission ( $300\ \mu\text{m}$  thick) detector backed by a  $1\ \text{mm}$  thick detector. The area of the telescope detectors is  $6 \times 4\ \text{cm}^2$ . The two evaporation residue trigger detectors are indicated as SI1 and SI2 and are also  $300\ \mu\text{m}$  thick with a  $25\ \text{cm}^2$  area.

## II. EXPERIMENTAL DETAILS

The experiment was performed at the Cyclotron Institute of Texas A&M University.

The  $110\ \text{MeV}$   $^{11}\text{C}$  beam was produced by charge exchange reaction of a primary  $^{11}\text{B}$  beam at  $13\ \text{A MeV}$  on a  $\text{LN}_2$  cooled hydrogen gas target. The primary beam was accelerated by the K500 superconducting cyclotron.

The momentum achromatic recoil spectrometer (MARS) was used to select the  $^{11}\text{C}$  ions [9], suppressing unwanted beam contaminations and defining the secondary beam characteristics in terms of energy and angular emittance. After this selection, an average intensity of  $4 \times 10^5$  particles/s was obtained on the target positioned at the MARS focal plane.

The target, prepared by evaporation, was  $500\ \mu\text{g}/\text{cm}^2$  thick rubidium chloride, 98% enriched in  $^{87}\text{Rb}$ , deposited on a thin ( $15\ \mu\text{g}/\text{cm}^2$ )  $^{12}\text{C}$  backing.

The experimental setup used is schematically drawn in Fig. 1. Evaporation residues (ERs) were detected at forward angles ( $\theta_{\text{lab}}=9^\circ-19^\circ$ ) using two silicon detectors (indicated as SI1 LEFT and SI2 RIGHT in Fig. 1) of  $5 \times 5\ \text{cm}^2$  active area and  $300\ \mu\text{m}$  thick, placed at  $25\ \text{cm}$  from the target. The ERs from the  $^{11}\text{C}$ ,  $^{11}\text{B}+^{87}\text{Rb}$  reactions were identified by measuring their energies and times of flight (TOF) with respect to the cyclotron rf. In this way, discrimination against other reactions, such as fusion-evaporation on Cl and C nuclei contained in the target, was achieved.

The  $^{87}\text{Rb}$  target (indicated as T in Fig. 1) was positioned at the center of a close-packed silicon detector array (called in the following the SI-BARREL) for light charged particle measurement. The SI-BARREL covered about 30% of the total solid angle and consisted of six (B1 to B6 in Fig. 1) large area ( $5 \times 5\ \text{cm}^2$ ) Si detectors,  $300\ \mu\text{m}$  thick, and two telescopes both consisting of a  $300\ \mu\text{m}$  thick,  $6 \times 4\ \text{cm}^2$  transmission detector (S1 and S2 in Fig. 1) backed by a  $1000\ \mu\text{m}$  thick detector (M1 and M2 in Fig. 1). The trans-

mission detectors are divided into seven strips that provide angular distribution information.

In addition, three cylindrical BC501 liquid scintillators ( $12.5\ \text{cm}$  diameter and  $12.5\ \text{cm}$  length), were placed outside the scattering chamber at  $50\ \text{cm}$  from the target position, to detect the neutrons emitted in the reactions. Two of them were placed at  $\theta_{\text{lab}}=0^\circ$  and the third one at  $\theta_{\text{lab}}=45^\circ$  with respect to the beam direction. Pulse shape analysis was used to discriminate against the  $\gamma$  ray background.

In the  $^{11}\text{C}$ -induced reaction, we collected  $6 \times 10^6$  events triggered by a single hit in one of the two evaporation residue detectors. Since the goal of the experiment was the comparison of particle yields from the two isobaric nuclei  $^{98}\text{Mo}$  and  $^{98}\text{Tc}$ , a secondary  $^{11}\text{B}$  beam at  $110\ \text{MeV}$  was also produced by using the inelastic scattering of the primary beam on a hydrogen target and selecting the energy of scattered ions with MARS. In this way, the same experimental setup was used to study both reactions and the comparison of the experimental results can be performed directly. In the  $^{11}\text{B}$ -induced reaction,  $3 \times 10^6$  events with the same trigger condition were collected.

## III. EXPERIMENTAL RESULTS

In the data analysis, the first requirement was the discrimination of the evaporation residues produced in the reactions of the  $^{11}\text{C}/^{11}\text{B}$  beams with the  $^{87}\text{Rb}$  nuclei from other products, in particular from the background of evaporation residues produced in the fusion reactions on Cl and C nuclei contained in the target. This was achieved by using a TOF window corresponding to  $30-60\ \text{ns}$  flight time and selecting events having energies lower than  $12\ \text{MeV}$ .

The measured  $A \sim 98$  residue energies are below  $12\ \text{MeV}$  because pulse height defects in silicon detectors are large. A typical TOF versus energy scatter plot for evaporation residue singles is reported in Fig. 2.

To demonstrate that the right evaporation residues are selected in this way, we present in Fig. 3 the energy spectrum of ER in coincidence with charged particles detected in the backward part of the SI-BARREL. The experimental distribution is compared in Fig. 3 with results of a simulation performed by the Monte Carlo version [10] of the statistical model code CASCADE [11] (MCSM), where the geometry of the present experiment was properly taken into account.

Standard input parameters have been used in these MCSM calculations, including the level density parameter  $a=A/8\ \text{MeV}^{-1}$ , as suggested from previous experimental results in this mass region and at the same excitation energy [12,13]. The predicted ER energies were also corrected by subtracting the pulse height defects in the silicon detectors, calculated using the prescription from Refs. [14,15]. The agreement between the simulation and experiment is fair, reflecting the difficulties in taking into account all energy losses and pulse height defects for the low-energy residues in the  $^{87}\text{Rb}$  target itself and in the silicon detector. Nevertheless, the comparison in Fig. 3 provides a clear demonstration that the evaporation residues from the reactions with  $^{87}\text{Rb}$  nuclei have been properly selected.

Using the same ER gating conditions, the energy spectra of coincident light particles were obtained. Due to the low

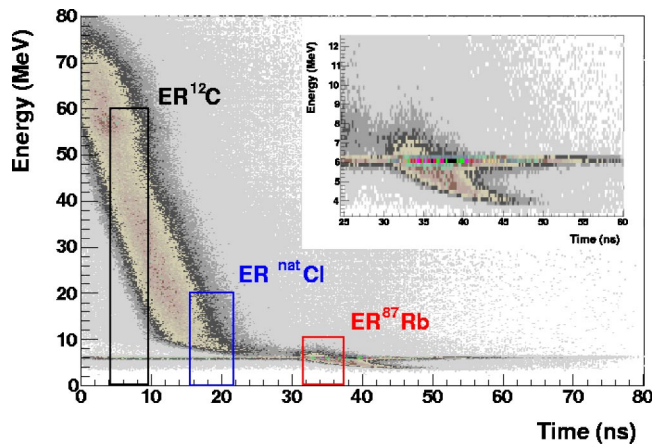


FIG. 2. (Color online) A typical time-of-flight vs energy scatter plot for the reaction products from the bombardment of the  $^{11}\text{C}$  beam on the  $\text{RbCl}(\text{C})$  target. The expected regions for residues from the different target nuclei are also indicated. In the inset, the region of evaporation residues from the reaction on the Rb target is shown. Events at about  $E=6$  MeV, randomly distributed in time, are due to a weak  $^{252}\text{Cf}$  source that was used to monitor the silicon triggers during the data taking.

statistics, only two spectra were derived by summing all events detected in the forward ( $\theta_{\text{lab}}=28^\circ-80^\circ$ ) or in the backward ( $\theta_{\text{lab}}=99^\circ-152^\circ$ ) parts of the SI-BARREL (including the  $\Delta E$  detector of the two telescopes S1 and S2), respectively. Such spectra are reported in Fig. 4 for the two reactions. It is seen that most protons punch through the silicon detectors, while lower energy  $\alpha$  particles are fully stopped. As a result, the spectrum exhibits a well-defined peak due to the protons and a broad distribution associated with the  $\alpha$  particles. The comparison with the MCSM simulation is also shown, in which the angular distribution of the emitted particles and related angle-dependent energy loss in the detectors were taken properly into account.

The total predicted spectra reported in Fig. 4 were obtained by separately normalizing the calculated proton and  $\alpha$  particle energy distributions to the experimental data in selected energy regions. This unfolding of the measured particle spectra relies on the predictive power of the MCSM which is well documented at this bombarding energy. The possibility of contributions from nuclear species other than proton and  $\alpha$  particles will be discussed in the following. The agreement between the experimental and predicted distributions is rather good, taking into account that we have integrated over a large angular range. Predicted energy distributions for proton and  $\alpha$  particles were, in turn, used to unfold from each experimental spectrum the yields for proton and  $\alpha$  particles and from that the angle integrated yield values.

The number of neutrons detected in coincidence with residues was obtained by analyzing the events in the BC501 scintillators. In this analysis, pulse shape discrimination was employed to reduce the  $\gamma$  ray background. Finally, events in all three detectors were summed, producing the neutron spectrum which is reported, as an example, in Fig. 5 for the  $^{11}\text{C}$  induced reaction case. The comparison between the experimental and MCSM predicted energy spectrum is more difficult in the neutron case, due to the need to correct not

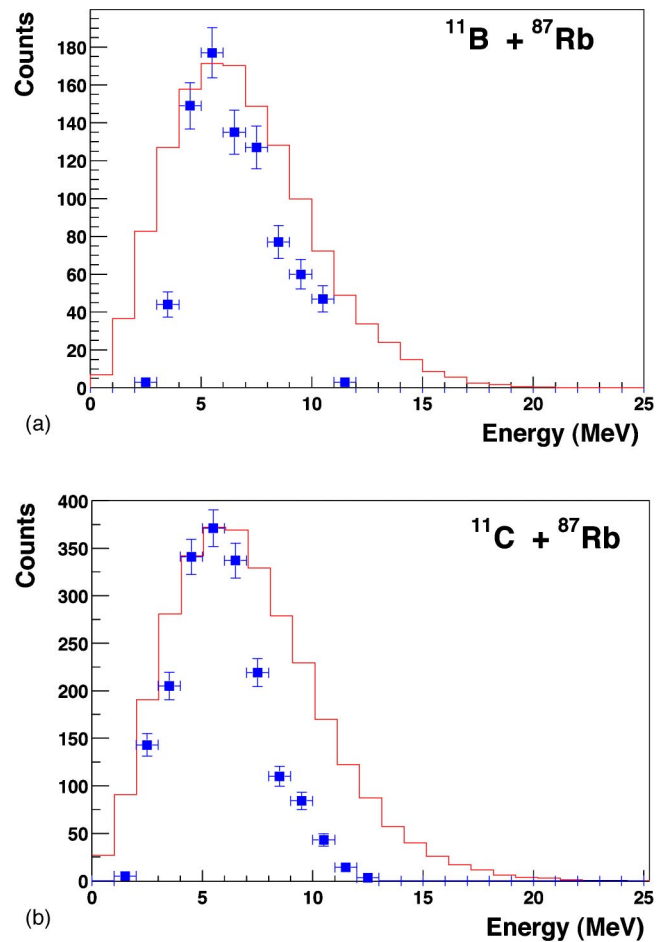


FIG. 3. (Color online) Typical ER energy spectra obtained for the residue-charged particle coincidence for the  $^{11}\text{B}$  beam (upper part) and the  $^{11}\text{C}$  beam (lower part) detected in the backward part of the SI-BARREL for a TOF window corresponding to 30–60 ns flight time.

only for the detector efficiency but also for attenuation and scattering in the reaction chamber walls. Because of the low statistics of the experimental spectra, we chose to use the neutron information in a simplified way. First, we derive directly the average time of flight associated with the detected neutrons and, from this value, the average neutron energy. The experimental average energy of neutrons is about 3 MeV, in good agreement with the value predicted from the MCSM simulations. After this test, the MCSM simulations were used to extract from the number of neutron events in the detectors, the angle integrated yield. The relative normalization factor between the two data sets for  $^{11}\text{B}$  and  $^{11}\text{C}$  beams was obtained from the total yield of single events in the trigger detectors, thus allowing a direct comparison between the neutron yield in the two reactions without any correction for detector efficiency and scattering and attenuation in the surrounding materials.

As a first test of the experimental results, we have compared the yield of charged particles detected in the two parts of the SI-BARREL. MCSM calculations predict that the ratio between the particle yield detected in the forward and backward parts of the barrel should be close to 1, as expected

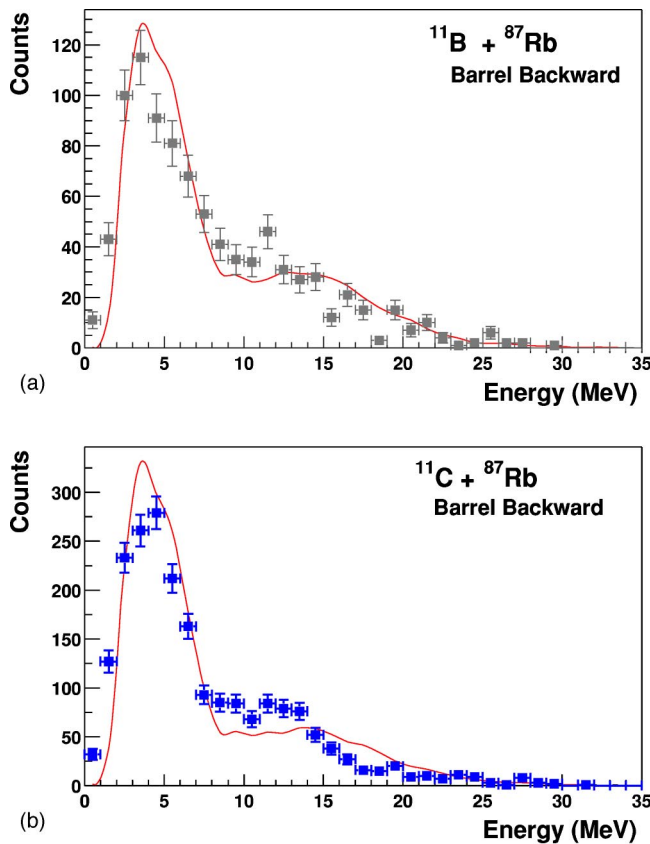


FIG. 4. (Color online) Spectra of the charged particles in coincidence with the ER for the 110 MeV for the  $^{11}\text{B}$  beam (upper part) and the  $^{11}\text{C}$  beam (lower part) on a  $^{87}\text{Rb}$  target.

from the decay of a fully equilibrated system characterized by a low velocity in the laboratory frame. Deviation from this expectation might be due to contributions from other reaction mechanisms such as the incomplete fusion and/or projectile breakup reactions that are expected to depend both upon the projectile type and on the specific light particle detected.

The experimental data reveal that in the case of the  $^{11}\text{B}$  beam, the forward to backward ratio for protons is  $R_{FB} \sim 1$ , in agreement with statistical model predictions. This is not the case for the  $\alpha$  particles, for which we found  $R_{FB} = 1.4$ . In the case of the  $^{11}\text{C}$  beam, the value  $R_{FB} \sim 0.7$  is found for both  $\alpha$  particles and protons. The deviations of  $R_{FB}$  from the predicted value, as in the  $^{11}\text{C}$  case, might be simply due to trivial experimental effects that decrease the yield of all forward emitted particles. In the case of the  $^{11}\text{B}$  beam, the difference between proton and  $\alpha$  particle ratios does, on the contrary, suggest that there is an extra yield of  $\alpha$  particles at forward angles. We take this observation as evidence that the  $^{11}\text{B}$  forward data are probably contaminated by incomplete fusion reactions initiated by the breakup of the  $^{11}\text{B}$  in a  $^4\text{He} + ^7\text{Li}$  pair that cannot be suppressed by the gate used to tag the ER. This possibility was confirmed by performing MCSM simulations in which several projectile breakup reactions followed by complete fusion of part of the projectile were investigated.

The issue of the incomplete fusion is rather complex. On the one hand, the presence of an incomplete fusion compo-

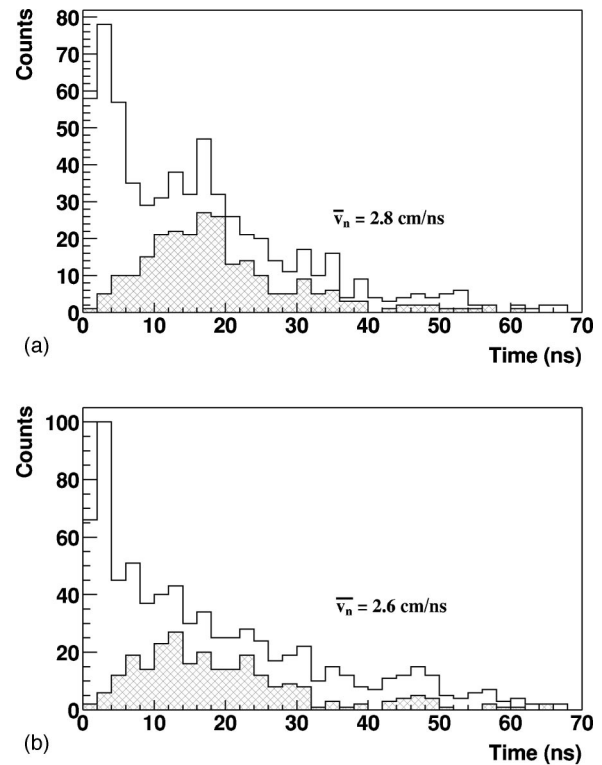


FIG. 5. Typical time-of-flight neutron spectra in coincidence with the ER for the 110 MeV  $^{11}\text{B}$  beam (upper part) and the  $^{11}\text{C}$  beam (lower part) on a  $^{87}\text{Rb}$  target, with (dashed area) and without the suppression of the  $\gamma$  background operated by means of the pulse shape analysis.

nent is also already documented with light heavy ion beams at bombarding energies comparable to those of this work [16–18]. On the other hand, a recent measurement of the excitation functions for the reactions  $^{197}\text{Au}(^{11}\text{C}, xn)$  and  $^{197}\text{Au}(^{12}\text{C}, xn)$  have been measured up to the bombarding energy of this work [19]. The obtained experimental results have been satisfactorily reproduced using fusion-evaporation models assuming complete fusion. This latter fact is consistent with our observation that, with the  $^{11}\text{C}$  beam, there is no evidence for contamination of the data from other reaction mechanisms.

Nevertheless, in the following analysis we have used only the data from the backward part of the SI-BARREL. Selection of these data is assumed to better reflect the decay of the compound nucleus populated in the fusion reaction and to minimize the contribution from projectile breakup [20].

Furthermore, we note that the statistical uncertainties associated with the experimental results are not negligible. Consequently we present the final charged particle data simply in terms of ratios between proton and  $\alpha$  multiplicities for each reaction, to avoid additional uncertainties associated with the absolute normalization of the experimental spectra. The only additional uncertainties to be taken into account are then related to the possibility of a component in the spectrum due to the  $^2\text{H}$ ,  $^3\text{H}$ , or  $^3\text{He}$  evaporation that cannot be evidenced in our technique of spectral unfolding. A  $^2\text{H}$  contribution cannot, indeed, be disregarded, as documented from the results reported in Ref. [13]. This implies a further 5%

additional uncertainty in the determination of the proton yields.

With this uncertainty, the relative proton and  $\alpha$  multiplicities were extracted from the measured backward angle spectra with the help of the MCSM predictions yielding  $M_p/M_\alpha=0.94\pm 0.06$  for the  $^{11}\text{C}$ -induced reaction and  $M_p/M_\alpha=0.68\pm 0.06$  for the  $^{11}\text{B}$ -induced reaction, respectively. For the neutrons, the ratio of the multiplicities measured with the two different beams  $M_n(^{11}\text{B})/M_n(^{11}\text{C})=1.26\pm 0.13$  will be directly considered in the following discussion.

#### IV. STATISTICAL MODEL CALCULATIONS

To search for temperature dependent effects, we have performed a systematic comparison between statistical model predictions and the experimental results. To study the sensitivity of the statistical model calculations to the different input parameters, the analytical version of the CASCADE code has been used. To avoid ambiguities in the results of the statistical model calculation, we studied the sensitivity of predictions, and thus their deviations from the experimental data, by tuning one input parameter at a time. In particular, we focused our attention on those parameters that are known to be effective in determining the particle multiplicities: the level density parameter  $a=A/K$ , the transmission coefficients  $T_l$ , and the binding energies  $B$ . Several previous works were devoted to the study of the properties of hot nuclei by comparing experimental particle spectra and multiplicities with CASCADE calculations in the same mass and excitation energy range [12,13,18]. These earlier results have been used as a guide in the present study.

##### A. The level density parameter

The first set of calculations was performed using standard masses for  $T=0$  MeV nuclei [21] and the so-called ‘‘spherical’’ transmission coefficients derived from the optical model potentials [22], but varying the level density parameter  $a=A/K$  in the range  $K=7-12$  MeV. In those calculations, the level density parameter is assumed to be constant with excitation energy and the same parameter was used for all the nuclei in the deexcitation cascade.

As shown in previous works [4–6], the level density parameter  $a$  decreases from its ‘‘cold’’ standard value  $A/8$  MeV $^{-1}$  as the excitation energy increases because of the temperature dependence of the nucleon effective mass. Such a decrease has been experimentally evidenced even if a constant, average level density parameter  $a_{ave}=A/\langle K \rangle$  is used in the calculation along all the deexcitation cascade [5,12]. The results of our calculations, showing the comparison between the experimental charged particle multiplicity ratio and those of the calculations, are reported in Fig. 6. The deviation from the experimental values,  $\Delta=[(\text{Calc}-\text{Exp})/\text{Calc}]$ , is  $\Delta=30\%$  ( $\Delta=22\%$ ) in the  $^{11}\text{B}$  ( $^{11}\text{C}$ ) case, when the standard level density ( $K=8$  MeV) value is used. The deviations decrease significantly well below the  $\Delta=10\%$  level for calculations using level density inverse parameters around  $a=A/11$  MeV $^{-1}$ . Furthermore, the predicted neutron multiplicity ratio

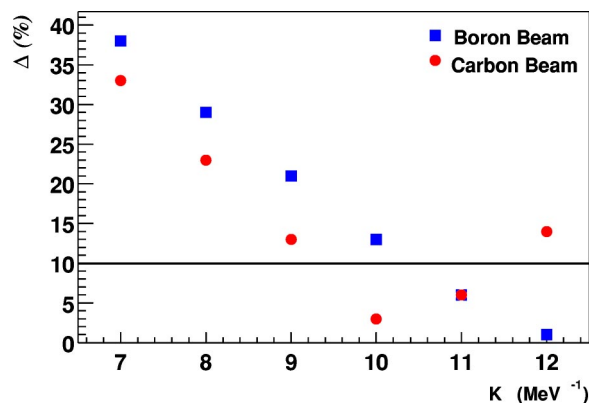


FIG. 6. (Color online) Comparison of experimental result for the proton to  $\alpha$  particle ratio and predictions from statistical model calculations with different level density parameters. The relative deviation  $\Delta$  is reported. For details see the text.

$M_n(^{11}\text{B})/M_n(^{11}\text{C})$  is very close to the experimental value ( $\Delta=8\%$ ) for all the level density values in the explored range.

The results obtained are qualitatively in agreement with expectations based on the temperature dependence of the nucleon effective mass. It has, however, to be noted that the use of the parameter value around  $a=A/11$  MeV $^{-1}$  is in conflict with past results for  $^{98}\text{Ru}$  compound nuclei populated in the same excitation energy region [13]. In that case, absolute  $p$  and  $\alpha$  particle multiplicities and energy spectra were described by CASCADE calculations in which the standard  $a=A/8$  MeV $^{-1}$  parameter was employed. We stress the fact that the high-energy slope of the particle spectra are very sensitive to the level density so that high statistics experimental energy spectra can be used as in Ref. [13] to determine the best value of the level density parameter.

Isospin dependent parametrizations for the level density have recently been proposed [23], suggesting values of about  $K=9-10$  for the nuclei of interest in this work. CASCADE calculations including such a parametrization lead to multiplicity values comparable to those obtained with a constant level density parameter  $a=A/10$  MeV $^{-1}$  for all nuclei in the decay cascade. A significant test of the proposed parametrizations will need again a comparison with high statistics particle spectra.

##### B. The emission barrier

The transmission coefficients are generally calculated by considering the optical model potentials describing the inverse capture reaction on cold nuclei, with the assumption that the emission barriers for cold and hot nuclei are identical. It is found that, in most cases, the reference calculations are not able to describe the experimental data [24]. In particular, deviations between experimental and calculated spectra at low particle energy have been taken in the past as an indication of significant differences in shape or size between hot and cold nuclei. Consequently, the parameters of the calculations are often adjusted to simulate changes in size and/or shape of the emitter that are assumed to be driven by the angular momentum [25].

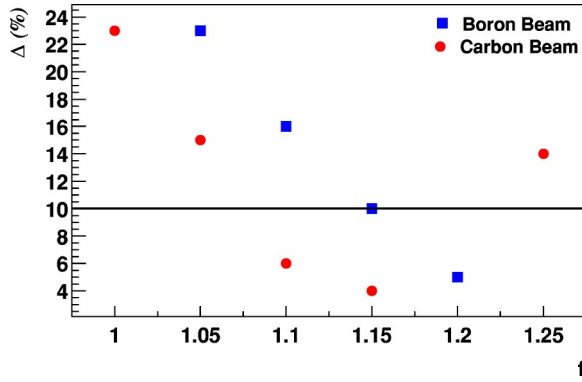


FIG. 7. (Color online) Comparison of experimental result for the proton to  $\alpha$  particle ratio and predictions from statistical model calculations with different transmission coefficients. The relative deviation  $\Delta$  is reported. For details see the text.

A simple way to adjust the emission barrier is to increase the optical model radius  $R_{OM}$  by a multiplication factor  $f$ , thus obtaining an effective radius  $R=f \times R_{OM}$  [26]. In the present case, we have performed statistical model calculations in which multiplication factors ranging from  $f=1.00$  to  $f=1.25$  were considered. In such calculations standard  $T=0$  MeV masses and level density parameter value  $a=A/8$  MeV $^{-1}$  were used. The results are reported in Fig. 7. It appears that a very good description of the proton to  $\alpha$  particle multiplicity ratio is obtained with an effective radius  $R=1.15 \times R_{OM}$ . For this  $R$  value, deviations between experimental and calculated proton to  $\alpha$  multiplicity ratio are again below  $\Delta=10\%$ . Also in this case, the neutron data are found to be rather insensitive to the variation of the optical model potential parameters ( $\Delta=8\%$  for all  $R$  values considered). The 15% expansion of the optical model radius quoted in this work is in agreement with past experiments [12,13,26,27], in which nuclei at about 100 MeV excitation energy were populated.

It should also be noted that the comparison between experimental data and calculations reported in Fig. 7 seems to indicate the need of a slightly different optical model effective radius to fit the data obtained in the two reactions. It has been suggested, indeed, that the emission barrier for particle evaporation would also depend on the  $N/Z$  ratio of the specific decaying nucleus, because of the isospin dependence of the nuclear radius [28]. This suggests that the  $^{98}\text{Tc}$  radius should be slightly larger than the  $^{98}\text{Mo}$  one. However, the above predicted nuclear radius variation for the two nuclei is only of the order of 0.4%, whereas the comparison with the experimental data would suggest a difference of about 5%.

### C. The binding energy

The last series of calculations was performed to explore the effects due to the predicted temperature dependence of the nuclear binding energy. It is expected, indeed, that the change of the binding energy will modify the energetic cost for the emission of each particle, thus modifying the deexcitation cascade. Since the temperature dependence of the binding energy is predicted to be isospin dependent, it is

further expected that such effects should depend on the  $N/Z$  ratio of the studied compound nucleus.

As a first step, the mass formula proposed by Pi, Vinas, and Barranco [8] was introduced in the CASCADE code. In this formula the binding energy is parametrized as a function of the mass and atomic numbers ( $A, Z$ ) and of the nuclear temperature  $T$ :

$$\frac{B}{A} = (a_v + \alpha_v T^2) + (a_s + \alpha_s T^2) A^{-1/3} + (a_{sym} + \alpha_{sym} T^2) \frac{I^2}{A^2} - \left[ \frac{3}{5} \frac{e^2}{r_0} \left( 1 - \frac{\alpha_{coul}}{A^{2/3}} \right) + \alpha_{coul} T^2 \right] \frac{Z^2}{A^{4/3}} + (a_{ss} + \alpha_{ss} T^2) \frac{I^2}{A^{7/3}}. \quad (1)$$

In Ref. [8], the numerical values of the parameters are provided to compute volume ( $a_v, \alpha_v$ ), surface ( $a_s, \alpha_s$ ), Coulomb ( $a_c, \alpha_c$ ), symmetry ( $a_{sym}, \alpha_{sym}$ ), and surface symmetry ( $a_{ss}, \alpha_{ss}$ ) contributions as well as the pairing correction ( $\Delta$ ) to the total binding energy. We stress the fact that this is the only formula available in literature that provides a full temperature dependence of the binding energies for all nuclear masses. On the contrary, the predictions of Donati *et al.*, reported in Ref. [7], refer to specific nuclei (e.g.,  $^{98}\text{Mo}$ ), and provide numerical results only for the symmetry energy contribution to the binding energy.

The Pi, Vinas, and Barranco formula was used to calculate the binding energies at  $T=2$  MeV, i.e., the temperature value that roughly corresponds to the average excitation energy along the deexcitation cascade for the reactions studied in this work. CASCADE calculations were performed using these binding energies together with a level density parameter  $a=A/8$  MeV $^{-1}$  and standard optical model transmission coefficients. Results of these calculations yield a deviation  $\Delta=10\%$  for the proton to  $\alpha$  particle multiplicity ratio in case of the  $^{11}\text{B}$  induced reaction. This is much better than the deviation obtained with the standard calculations in which  $T=0$  MeV binding energies are employed. However, following the same procedure for the  $^{11}\text{C}$  induced reaction, the description of the experimental results is very poor, being the observed deviation  $\Delta=77\%$ . This demonstrates how large is the effect of the isospin differences in such model predictions.

We stress the fact that the Pi, Vinas, and Barranco formula offers a detailed prediction of the temperature effect applicable in the full mass range sampled in this experiment. In contrast, Donati's predictions reported in Ref. [7] refer only to  $^{98}\text{Mo}$  being not clear if this correction should be applied for all nuclei involved in our deexcitation cascade. Moreover, it is also not clear in this case how to handle the temperature dependence of the other terms (Coulomb, surface, and volume), which are also expected to be temperature dependent, as in the work of Ref. [8].

As a final test, we have included in the calculations the correction of Donati *et al.* to the symmetry energy term of the binding energy. This has been done using the  $b_{sym}(T)$  value for the  $^{98}\text{Mo}$  nucleus provided in Ref. [7] at the average nuclear temperature  $T=2$  MeV and scaling the correction as  $E_{sym}=b_{sym}[(N-Z)^2/A]$  for the nuclei populated in the

decay cascade. The temperature dependence of the other terms (i.e., Coulomb, surface, and volume) was disregarded. Such calculations lead to very large deviations with respect to the experimental data. In particular, the deviation is about  $\Delta=80\%$  when the correction is applied to all nuclei along the deexcitation cascade. This value decreases to  $\Delta=40\%$  ( $50\%$ ) for  $^{11}\text{B}$  ( $^{11}\text{C}$ ) case if this correction is applied only in the first decay step, i.e., emission from  $^{98}\text{Mo}$  ( $^{98}\text{Tc}$ ) only.

## V. SUMMARY AND CONCLUSIONS

The use of radioactive beams is now opening several new possibilities in nuclear physics studied with heavy ion beams. Particularly appealing is the possibility to explore isospin related effects on the formation and decay of hot nuclei. In this respect, we have presented in this work results obtained in a comparative study of the decay of the two isobars  $^{98}\text{Mo}$  and  $^{98}\text{Tc}$  populated by fusion reactions of 110 MeV  $^{11}\text{B}$  and  $^{11}\text{C}$  beams on a  $^{87}\text{Rb}$  target.

This work was motivated primarily by theoretical predictions suggesting that the binding energy is a function not only of the nuclear temperature  $T$ , but also of the  $N/Z$  ratio in a given nucleus. A consistent formula describing in detail the temperature dependence of the binding energy was proposed several years ago by Pi, Vinas, and Barranco [8]. Recently, temperature effects in specific nuclei relevant for nuclear astrophysics, were studied by Donati *et al.* [7]. Sizable variations of the symmetry energy were suggested. Such predictions have been also confirmed by an independent study on the same nuclei by Dean *et al.* using Monte Carlo shell model calculations [29]. The dependence of the binding energy on the temperature and isospin is expected to have a significant effect in determining the de-excitation cascade, particularly in the multiplicities of the emitted particles. As a matter of fact, standard statistical model calculations predict a sizable change in the particle multiplicities when the temperature and isospin [8] dependence of the binding energy is properly taken into account, even when a modest isospin change such as the one obtained in the present experiment is considered.

The results presented in this work, consisting mainly of proton to  $\alpha$  particle multiplicity ratios for the two reactions, are compared with statistical model calculations using both standard and adjusted parameters. In the comparison, backward emitted particles have been considered, to minimize the possible contamination from projectile breakup in the measured spectra. Generally, the agreement between calculations with standard parameters and experimental data is fair, without a marked dependence on the beam which resulted by the inclusion in the model calculation of the temperature and isospin dependent binding energies from Ref. [8]. The agreement is improved significantly by slight modifications of the transmission coefficients, consistently with past particle evaporation studies in this mass region [12,13,27].

Within the limits of the present investigation, the experimental results do not show the need for inclusion of the

predicted temperature and isospin related effects on the binding energy in the statistical model calculations.

We stress the fact that the level density parameter dependence on the  $N/Z$  ratio of the nucleus has been recently studied [23]. Moreover, it has also been suggested that the barriers for particle evaporation from specific nuclei will also depend on the  $N/Z$  ratio, because of the isospin dependence of the nuclear radius [28]. It is worth mentioning that Charity *et al.* [30] have recently reported on a detailed investigation of the  $^{92,100}\text{Mo}+^{60}\text{Ni}$  fusion evaporation reaction. Also in this work it is not found necessary to employ an isospin dependence of the level density. However, despite the results obtained in such investigations, the search for  $N/Z$  dependent effects is an interesting research field that needs to be further pursued experimentally, when more exotic projectiles with larger isospin differences become available at future radioactive ion beam facilities. The possibility of the detection of isospin effects is strictly correlated to the selected reactions, to the measured quantities and to the experimental accuracy. The latter point depends mainly on the intensity of the available radioactive beams. The selection of suitable reactions and sensitive experimental observables is also of paramount importance for such experimental investigations. In particular, the use of light beams such as  $^{11}\text{B}$  and  $^{11}\text{C}$ , employed in the present experiment, has the advantage of populating the compound nucleus at relatively low spin, thus reducing angular momentum induced effects. On the other hand, in the case of light beams, a possible contamination from incomplete fusion reactions and/or projectile breakup has to be taken into account.

Finally, it is important to stress that the different predicted effects (i.e., changes of the binding energies, level densities, and/or emission barriers) might be studied in future investigations by looking not only at the proton to  $\alpha$  particle multiplicity ratio, as done in the present experiment, but also at the energy spectra of the emitted particles. It is known that different energy regions in the particle spectra can be used to get information on the barrier (low energy part of the spectrum) and on level density (high-energy slope of the particle spectrum). The study of exclusive particle spectra in reactions induced by radioactive beams requires a substantial increase in the integrated RIB intensity and the availability of more powerful detection systems. Thus it will be more easily obtained in the next generation of RIB facilities.

## ACKNOWLEDGMENTS

Many thanks are due to the Cyclotron Institute staff for the technical support during the experiment and to the accelerator crew for the smooth operation of the accelerator. The support of M. Caldogno during the setup and commissioning of the apparatus is acknowledged. We thank S. Shlomo and P.F. Bortignon for several useful discussions. The participation of G. LaRana and R. Moro in the earlier phases of this project is also acknowledged. This work was supported by INFN, by the U.S. Department of Energy, and by The Robert A. Welch Foundation.

- [1] See, for example, E. Suraud, Ch. Grégoire, and B. Tamain, *Prog. Part. Nucl. Phys.* **23**, 357 (1989).
- [2] P. F. Bortignon and C. Dasso, *Phys. Lett. B* **189**, 381 (1987), and references therein.
- [3] S. Shlomo and J. B. Natowitz, *Phys. Rev. C* **44**, 2878 (1991).
- [4] G. Nebbia *et al.*, *Phys. Lett. B* **176**, 20 (1986).
- [5] K. Hagel *et al.*, *Nucl. Phys.* **A486**, 429 (1988).
- [6] M. Gonin *et al.*, *Phys. Lett. B* **217**, 406 (1989).
- [7] P. Donati *et al.*, *Phys. Rev. Lett.* **72**, 2835 (1994).
- [8] M. Pi, X. Vinas, and M. Barranco, *Phys. Rev. C* **26**, 733 (1982).
- [9] A. M. Mukhamedzhanov *et al.*, *Phys. Rev. C* **66**, 027602 (2002), and references therein.
- [10] R. K. Choudhury *et al.*, *Phys. Lett.* **143B**, 74 (1984).
- [11] F. Puehlhofer, *Nucl. Phys.* **A280**, 267 (1977).
- [12] G. Nebbia *et al.*, *Nucl. Phys.* **A578**, 285 (1994).
- [13] M. Kildir *et al.*, *Phys. Rev. C* **46**, 2264 (1992).
- [14] G. Pasquali *et al.*, *Nucl. Instrum. Methods Phys. Res. A* **405**, 39 (1998).
- [15] G. Tabacaru *et al.*, *Nucl. Instrum. Methods Phys. Res. A* **428**, 379 (1999).
- [16] P. Vergani *et al.*, *Phys. Rev. C* **48**, 1815 (1993).
- [17] D. J. Parker *et al.*, *Phys. Rev. C* **44**, 1528 (1991).
- [18] M. Lunardon *et al.*, *Nucl. Phys.* **A652**, 3 (1999).
- [19] R. Joosten *et al.*, *Phys. Rev. Lett.* **84**, 5066 (2000).
- [20] See, for example, K. Hagel *et al.*, *Nucl. Phys.* **A486**, 429 (1988).
- [21] Liquid drop masses from W. D. Meyers and W. J. Swiatecki, *Ark. Fys.* **36**, 343 (1967).
- [22] For transmission coefficient calculations the following optical model parametrization was used: neutrons—D. Wilmore and P. E. Hodgson, *Nucl. Phys.* **55**, 673 (1964); protons—F. G. Perey *et al.*, *Phys. Rev.* **131**, 745 (1963);  $\alpha$  particles—J. R. Huizenga and G. Igo, *Nucl. Phys.* **29**, 462 (1961).
- [23] S. I Al-Quraishi *et al.*, *Phys. Rev. C* **63**, 065803 (2001).
- [24] See, for example, J. M. Alexander *et al.*, *Nuclear Dynamics and Nuclear Disassembly* (World Scientific, Singapore, 1990), p. 211, and references therein.
- [25] R. J. Charity, *Phys. Rev. C* **61**, 054614 (2000), and references therein.
- [26] B. Fornal *et al.*, *Phys. Rev. C* **42**, 1472 (1990).
- [27] Z. Majka *et al.*, *Phys. Rev. C* **35**, 2125 (1987).
- [28] K. Pomorski *et al.*, *Acta Phys. Pol. B* **28**, 413 (1997), and references therein.
- [29] D. J. Dean, K. Langanke, and J. M. Sampaio, *Phys. Rev. C* **66**, 045802 (2002).
- [30] R. J. Charity *et al.*, *Phys. Rev. C* **67**, 044611 (2003).